Food Bioscience 67 (2025) 106318

Contents lists available at ScienceDirect

Food Bioscience

journal homepage: www.elsevier.com/locate/fbio

Functional and antioxidant characteristics of the dietary fiber extracted from pearl millet

K.M. Manju [a], Swati Srivastava [b], Brij Pal Singh [a,c], Dheeraj Raya [b], Rohit [a], Rusli Fridyanto [d], Roni Ridwan [d], Yantyati Widyastuti [d,e], Teck Chwen Loh [f], Hooi Ling Foo [g], Saurabh Sudha Dhiman [b,h,*], Gunjan Goel [a,**]

[a] Department of Microbiology, School of Interdisciplinary and Applied Sciences, Central University of Haryana, Mahendergarh, 123031, India
[b] Civil and Environmental Engineering, South Dakota Mines, Rapid City, SD, 57701, USA
[c] University Centre for Research and Development (UCRD), Chandigarh University, Gharuan, Mohali, 140413, Punjab, India
[d] Research Center for Applied Zoology, National Research and Innovation Agency (BRIN), Indonesia
[e] Research Center for Animal Husbandry-National Research and Innovation Agency (BRIN), Cibinong 16911, Indonesia
[f] Department of Animal Science, Faculty of Agriculture, Universiti Putra Malaysia, 43400 UPM, Serdang, Selangor, Malaysia
[g] Department of Bioprocess Technology, Faculty of Biotechnology and Biomolecular Sciences, Universiti Putra Malaysia, 43400 UPM, Serdang, Selangor, Malaysia
[h] Chemistry, Biology and Health Sciences, South Dakota Mines, Rapid City SD 57701, USA

ARTICLE INFO

Keywords:
Antioxidants
Binding energy
dietary fibers
Flavonoids
Molecular simulations
Pearl millet
Probiotic index

ABSTRACT

The envisioned research aims to investigate the functional characteristics of pearl millet's dietary fiber to meet the growing demand for nutraceutical dietary fibers. Our results demonstrate that fiber extracted using various chemical-intensive and enzymatic methods possesses an impressive prebiotic index, cholesterol-absorbing capacity, and remarkable oil and water-holding capabilities (WHC), making it a valuable asset for the food processing industry. The fiber extracted through the alkali-mediated (alkSDF) approach demonstrated the highest WHC (9.22 g/g) compared to the lowest values (1.01 g/g) observed through enzymatic treatment. Likewise, the highest free radical scavenging activity (92%) using ABTS assay was noted for alkSDF, whereas the enzymatic approach exhibited the lowest antioxidant characteristics (11%). A comprehensive morphological analysis indicated smooth surface with acid extracted fiber as compared to rough surface and higher crystallinity obtained by alkali treatment. Specifically, dietary fiber obtained through amylase-assisted ultrasonication exhibits improved thermal properties and superior abilities to absorb glucose (7.53 mM/g) and cholesterol (1.43 mg/g). Moreover, *in-silico* analysis has revealed the crucial active site amino acids involved in amylose binding and substrate catalysis, facilitating the release of reducing sugars into the medium. The structural and functional properties of pearl millet fiber establish it as a highly effective and accessible food supplement for various biomedical applications.

1. Introduction

Dietary fibers are classified as plant material with several components, including noncellulosic polysaccharides, e.g., gums, mucilages, and non-carbohydrate components (Dhingra et al., 2012). Their resilient characteristics against various enzymatic reactions and antioxidant properties have garnered broad-spectrum applications in food processing (Palafox-Carlos et al., 2011). Due to their commercial potential, the global dietary fibers market size was USD 7.45 billion in 2023, accounting for USD 8.16 billion in 2024, and is expected to reach around USD 19.97 billion by 2034, expanding at a compound annual growth rate (CAGR) of 9.4% from 2024 to 2034 (Research, 2024). However, the supply-chain imbalance has recently loomed over the predicted CAGR of dietary fibers. Numerous reports have been published on deploying enzymatic-gravimetric (Asp, 1987), chelation-based (Tejada-Ortigoza et al., 2020), and more (Wang et al., 2022) to extract dietary fibers

This article is part of a special issue entitled: Bioproducts and functional food published in Food Bioscience.

* Corresponding author. Civil and Environmental Engineering, South Dakota Mines, Rapid City, SD, 57701, USA.
** Corresponding author.
E-mail addresses: Saurabh.dhiman@sdsmt.edu (S.S. Dhiman), gunjanmicro@gmail.com (G. Goel).

https://doi.org/10.1016/j.fbio.2025.106318
Received 22 December 2024; Received in revised form 4 March 2025; Accepted 6 March 2025
Available online 7 March 2025

efficiently to maintain such a delicate balance of supply chain scenarios. Although published reports validate the role of a specific methodology in extracting dietary fiber, experimental advantages over other reported techniques have not been discussed comprehensively.

Like the myriad extraction methodologies deployed, various substrates and biomass types, e.g., plant-based waste (Buljeta et al., 2023), mushroom (Jia et al., 2020), fruit waste, seed (Feng et al., 2024), and more (Okrathok et al., 2022), have also been investigated for dietary fiber extraction. Considering the biomedical applications of dietary fibers (Yang et al., 2017), it is quintessential to exhaustively screen the biomass types, including underutilized crops growing in semi-dry and salt-affected areas (Lin et al., 2022). One such example is *Pennisetum glaucum* var. Dhania (*aka* pearl millet) that shows a low glycemic index (Pei et al., 2022) and high fiber contents (~7/100g) (Agrawal et al., 2023), making it a promising biomass after buckwheat millet (Sofi et al., 2023) for extracting dietary fibers. Remarkably, the nutrient compositions, i.e., protein (14.5%), crude fiber (2.0%), etc., of pearl millet are comparable to the popular grains (e.g., wheat, rice) (Devi et al., 2014). Additionally, its antioxidant characteristics will be vital for treating metabolic diseases by maintaining a healthy gut microbiota (Bala Durairajan et al., 2024; Pei et al., 2022).

Since the presence of phytates, polyphenols, and tannins in pearl millet has already been confirmed, it is imperative to correlate their presence with antioxidant activities. Because phenolics are not equally distributed in the grain and are mainly concentrated in the outer layers (Happi Emaga et al., 2008), it is vital to standardize the extraction methodologies, resulting in the highest yield of the polyphenols with their intact chemical structures. Considering that phenolic compounds primarily exist as soluble conjugates, soluble fractions of the dietary fibers are important parameters for evaluating the efficiency of any adopted extraction methodology (de Simas et al., 2010). Most of the phenolic compounds in the millet exist in the form of glycosides (Hilu et al., 1978). However, reports are available on ferulic acid as the major bound phenolic acid and protocatechuic acid as the major free phenolic acid of the millet (Subba Rao & Muralikrishna, 2002). The presence of ferulic acid is important as its concentration can be used as a standard compound to measure the total phenol concentration of the selected biomass.

Considering the status quo of India as the largest producer of pearl millet in the world (Agrawal et al., 2016) and the availability of extensive information on mineral accessibility of dietary fibers, in-depth characterization of functional and antioxidant properties of pearl millet will be vital for developing novel functional foods leveraging the bioactive component. However, low bioactivity, poor aqueous solubility, and stringent metabolism are noteworthy challenges in characterizing the dietary fibers. In these challenging scenarios, molecular docking (Vijayakumar et al., 2020) has proven instrumental in deciphering the underlying mechanisms that determine the bioactive properties of dietary fibers (Elsafy et al., 2024). Likewise, high-performance analytical techniques (Coppin et al., 2013) for identifying the biofunctional constituents are vital in quantifying the flavonoid ratio.

To achieve the highest quantity of dietary fiber from pearl millet without compromising its bioactive properties and to decipher the underlying mechanisms governing the antioxidant characteristics, the current investigation aimed (i) a comparative analysis of the chemical and enzymatic extraction approaches, (ii) determination of the polyphenols associated antioxidant activities and other functional activities such as prebiotic index of the dietary fiber, and (iii) docking amylose as ligand to identify the key amino acids facilitating the release of dietary fibers.

2. Material and methods

2.1. Raw material and reagents

Fresh raw pearl millet grain was obtained from a local farm in Haryana, India. Before processing, the raw material was screened and filtered through a 70 mm mesh sieve to eliminate cracked grains and weeds. Under aseptic conditions, the milled flour was soaked in 85% (v/v) ethanol for 48 h to extract fat-soluble substances, rendering it fat-free, followed by drying at 40 °C. The dried slurry was stored at approximately 25 °C in airtight containers until further use. The commercial enzyme preparations, namely α-amylase (EC 3.2.1.1, sourced from hog pancreas), amyloglucosidase (EC 3.2.1.3, sourced from *Aspergillus niger*), and protease (EC 3.4.21.62, sourced from *Bacillus licheniformis*), were purchased from Sigma Aldrich. All other chemicals and reagents were of high analytical grade.

2.2. Dietary fiber extraction methodologies

2.2.1. Acid and alkali-mediated fiber extraction

For acid extraction of the DF, 20 g of fat-free pearl millet flour was mixed with 400 mL distilled water, and the pH was adjusted to 2.0 using 12M sulphuric acid (Fidriyanto et al., 2024). This mixture was stirred at 80 °C for 4 h in a water bath, followed by centrifugation at 5000*g* (15 min at 30 °C) and ethanol (95% v/v) mediated separation of the soluble fraction. A follow-up incubation of 1 h at 30 °C yielded a fraction of acid-soluble dietary fiber (AC-SDF). The insoluble residues were rinsed with distilled water until a neutral pH was observed, followed by oven drying (50 °C) to produce acid-extracted insoluble dietary fiber (AC-IDF). For alkali mediated extraction, the fat-free pearl millet flour (10 g) was soaked in 400 mL NaOH (1:40 w/v) at 30 °C for 3 h followed by the centrifugation (5000 g, 5 min, 4 °C) to separate SDF and IDF (Ding et al., 2020). The alkali soluble (AL-SDF) fractions were precipitated using 95% (v/v) ethanol and insoluble fraction was obtained as described above. Both the fractions were oven dried (50 °C) and preserved at 4 °C.

2.2.2. Enzymatic approach of fiber extraction

The enzymatic extraction of the dietary fiber was accomplished using the method described for soluble (Karimi et al., 2018) and insoluble (Wang et al., 2020) fractions. For extracting the soluble fraction of dietary fiber, α-amylase (~150 U/mg protein) was added to pearl millet and incubated at 75 °C for 1.5 h. The settled material was treated with 2 M acetic acid to maintain a pH of 3.5. After enzyme denaturation (boiling at 100 °C for 1h), 95% (v/v) ethanol was used for fiber extraction through precipitation. For extracting the insoluble fraction, fat-free pearl millet flour was sequentially treated with α-amylase (~150 U/mg protein), followed by protease (500 μL), and finally with amyloglucosidase (200 μL) at 40 °C for 1.5 h. The treated residues were washed twice with distilled water and dried at 25 °C.

2.2.3. Ultrasounication followed by enzymatic extraction

The pearl millet substrate was activated by ultrasonication before any enzymatic treatment (Calcio Gaudino et al., 2022). The sample (10 g) was mixed with distilled water, and pH was adjusted to 9.5 with continuous shaking for 1 h at 20 °C. The suspension was sonicated using an ultrasonic cleanser (LABWAN, Model no. LW-UC-12L) at 25 °C for 15 min with 40% amplitude. The adopted extraction methodologies for soluble and insoluble fractions are similar to those described for the enzymatic approach. All fractions of the dietary fibers were stored at 4 °C until further use.

2.3. Structural, surface, and stability characterization of fiber

The Fourier transform infrared (FTIR) spectra (Bruker Alpha II spectrometer) were used to determine the functional groups representing the spectroscopic features of different dietary fiber fractions. The wavelength for the analysis ranged between 400 and 4000 cm^{-1} with 32 scans (Chylińska et al., 2016).

The crystallinity of the fiber's fractions was determined using X-ray diffraction (XRD) patterns involving Cu-Kα radiation of samples and Θ-

compensated slit (20 mA, 30 kV) (Liu et al., 2019). The diffraction angle (2Θ) was performed scattering at 10–70 °C with a speed of 1 min^{-1}. The surface topology of the fiber's fractions coated with 10 nm gold powder was determined by scanning electron microscopy (SEM) (SU8100, HITACHI) at a 3.0 kV acceleration voltage analysis (Wang et al., 2022).

The thermal stability of extracted fractions was assessed using Differential Scanning Calorimetry (DSC) (Polyma DSC21400A, Germany). The dietary fiber samples (10 mg) were loaded in hermetic aluminum pans, and temperatures were scanned from 10 to 400 °C at a heating rate of 10 °C min^{-1} under nitrogen with a 10 mL min^{-1} flow rate (Tolve et al., 2024).

The surface topology of the DF fractions was determined by SEM (Model: SU8100, HITACHI, Japan) at a 3.0 kV acceleration voltage analysis. The samples under vacuum were placed on specimen holder that contained a dual-sided adhesive and then samples were coated using 10 nm gold powder using spray method and image were assessed using electron microscope.

2.4. Characterization of functional properties

The extracted fiber fractions were evaluaed for Cholesterol and glucose absorption capacity, water and oil hydration capacities, antioxidant and prebiotic activities as described below:

Fiber fraction (0.5 g, dry weight) was mixed with 25 mL diluted egg yolk (1:2 with H_2O) followed by pH adjustment (pH 7.0) and incubation (37 °C, 30 min, 200 rpm). After incubation, the mixture was centrifuged (3000 *g*, 10 min at 4 °C), and ~0.02 mL supernatant was collected and mixed with the 100 mL of glacial acetic acid and 2 mL H_2SO_4 (1 M) for its absorption analysis at 550 nm. The cholesterol adsorption capacity was calculated using the following equation:

$$\text{Cholesterol absorption capacity (mg/g)} = (Ab_{yolk} - Ab_{sample})/ \text{(dry weight of fiber)} \ldots. \quad (1)$$

For Glucose Absorption Capacity (GAC), 0.5 g (dry weight) of fiber fraction was mixed with 25 mL glucose (w/v) and incubated at 37 °C with continuous shaking (~200 rpm) for 6 h. After incubation, the mixture was centrifuged (4500 *g*, 10 min at 25 °C), and the supernatant was collected. To 1 mL of supernatant, 1 mL of phenol (5% w/v) and 5 mL of H_2SO_4 (98% v/v) were added, followed by additional incubation for 20 min (at 30 °C). The GAC was determined by taking the absorbance of the mixture at 480 nm and calculated using the following equation:

$$\text{Glucose absorption capacity (mM/g)} = (C_i - C_s) \times V_i / W_s \ldots. \quad (2)$$

C_i: Glucose concentration of 50 mM glucose; C_s: Glucose concentration of sample; V_i: Supernatant (1 mL); W_s: sample weight.

The water hydration capacity (WHC), oil holding capacity (OHC), and swelling capacity (SC) of each dietary fiber's preparation were determined according to the method previously described (Robertson et al., 2000).

The phenolic acid contents in the fiber fractions were determined as these contribute toward antioxidant activities. The pretreated millet samples were soaked in the minimal volume of sodium phosphate buffer (100 mM, pH 7.0) for 24 h at 25 °C to dissolve loosely bound phenolic compounds for HPLC-based detection (Chandrasekara & Shahidi, 2011). Before injection, all samples were filtered through a 0.2 μm membrane syringe filter (Whatman Inc., USA). The separation of phenolic compounds was carried out with the C_{18} column using a 1% formic acid (eluent A) and methanol/acetonitrile/formic acid (94:5:1; v/v/v) (eluent B) as mobile phase for HPLC (Agilent Technologies, USA). The gradient elution method was followed with a flow rate of 0.5 mL min^{-1}, and compounds were detected at 254 and 280 nm.

The free radical scavenging activities of all the fractions were determined using 2,2-azino-bis-3-ethylbenzothiazoline-6-sulphonic acid (ABTS) and ferric-reducing antioxidant power (FRAP) assays (Wang et al., 2021). In the case of FRAP assay, The standard curve was constructed using $FeSO_4$ solution (0.5–10 mg mL^{-1}). The results were expressed as the raw material's μmol Fe(II)/g-dry weight (Benzie & Strain, 1996).

The prebiotic activity (PI) of all the fractions was determined using the method described previously (Fidriyanto et al., 2023). Briefly, sugar free MRS base medium was supplemented with 2% of extracted fibre fraction individually and inoculated with activated standard probiotic strain *Lacticaseibacillus rhamnosus GG* (1.0×10^7 CFU/mL). The inoculated broth were incubated for 24 h at 37 °C and viable cell counts were determined on MRS agar. The Prebiotic Index (PI) was calculated according to Huebner et al. (2007) and compared with standard inulin as prebiotic substrate. A value greater than 1.0 for PI was considered as the substrate's positive effect on the proliferation of probiotics.

2.5. In-silico analysis

The homology model (Raya et al., 2022) for the α-amyloglucosidase enzyme was developed using the corresponding gene sequence in the whole genome of the *Aspergillus niger* in the JGI database. Multiple sequence alignment (Raya et al., 2023) was carried out to model the structure, which was further checked and superimposed with the PDB ID 2GVY as a template. The PROCHECK tool was used to cross-validate the authenticity and correctness of the modeled structure (Basotra et al., 2019). The structure of the ligand (amylose) was retrieved from the PubChem database in the SVF format. Candidate poses were created using random rigid-body rotations followed by simulated annealing. The protein structure was subjected to energy minimization using a CHARMM force field (Selvaraj et al., 2016). The candidate pose was selected based on the DOPE score and probability distribution field (PDF) energy values. The docked ligand orientation, which gave the lowest interaction energy, was selected for in-depth analysis of the active site environment and participating residue's stability. The Biovia Discovery Studio R2 licensed tool was deployed to simulate the protein structure, active site interactions, and energy calculations.

2.6. Statistical analysis

The data was analyzed using one-way analysis of variance (ANOVA) followed by Duncan's multiple-range test was employed to identify significant differences ($p < 0.05$). The statistical analysis was performed using SPSS (Version 23.0, SPSS Inc.) for all experiments performed in the triplicates.

3. Results and discussion

3.1. Effect of extraction methods on yield of dietary fibers

Numerous experiments were conducted under chemical-intensive and enzyme-catalyzed reaction conditions to achieve the highest quantity of fibers with robust surface properties (Fig. S1). In the case of the chemical-intensive methodologies, alkaline treatment resulted in the highest yield for the soluble fraction of the dietary fiber (*alk*SDF), followed by the insoluble fraction (*alk*IDF). The relatively lower yield of soluble (*ac*SDF) and insoluble (*ac*IDF) fractions of acid-treated pearl millet (Fig. S2) could be attributed to two major reasons: firstly, the conversion of hemicellulosic components in lower sugars or monosaccharides, and secondly, the destruction of the fragile monomeric structural elements into the unextractable byproducts (Bader Ul Ain et al., 2019). The acid-intensive methodology destroyed polysaccharides by breaking the glycosidic bonds and hydrolyzing the SDF into oligosaccharides and monosaccharides that cannot be precipitated (Lovegrove et al., 2017).

Due to the presence of hemicellulosic materials and lignin, appropriate enzymatic preparations—specifically α-amylase, amyloglucosidase, and protease—were utilized in combinations to enhance recovery efficiency. The enzymatic methodologies resulted in a lower yield of

dietary fibers (Fig. S2). This decreased yield may be attributed to the absence of pretreatment (Dhiman et al., 2017) or substrate activation (Dhiman et al., 2016) prior to enzyme application (Jagtap et al., 2014). A sequential methodology, such as a chemical-intensive pretreatment followed by enzyme application, was not performed due to the significant volume of clean water required for washing steps (Jagtap et al., 2013) and the toxicity of the furfurals (Kalyani et al., 2012) found in the resulting effluent. The motivation for adopting the UenzSD approach is to achieve structural disruption of the pearl millet biomass, thereby making the subsequent enzymatic treatment more efficient and enhancing the release of polysaccharides. However, the resilient fibrous seed coat structure (Pattanashetti et al., 2016), which is rich in fat, poses challenges in extracting dietary fibers even after ultrasonic pretreatment. As a result, a lower yield of approximately 1.5% was obtained through the UenzSDF approach (Fig. S2).

3.2. Structural, surface and stability characterization of fiber

The structural composition of dietary fibers observed through FTIR for all extracted samples is given in Fig. S1. The presence of an H-bond with hydroxyl or alcohol groups of polysaccharides from cellulosic components is validated by a strong peak of 3408–3445 cm^{-1} in all extracted samples (Skowron et al., 2020). Likewise, irrespective of extraction methodology type, the band corresponding to 1638-1640 cm^{-1} represented the β-sheet structures, and the peak at 1658 cm^{-1} represented the α-sheet structures. Additional peaks from 750 to 910 cm^{-1} validating the C-H bending of the syringyl unit, aromatic ring, and anti-symmetric out-phase ring stretching were also observed. The absorption peak corresponds to 2854-2961 cm^{-1}, representing the C-H bond stretching of carbohydrate methylene polysaccharides. A peak corresponding to 1400-1470 cm^{-1} was observed for CH_3 asymmetric vibration. The peak corresponding to 1500 cm^{-1} confirms the stretching vibration of aromatic rings in lignin in all the samples except the *ac*SDF. Additional peaks, viz. 1745 cm^{-1} in *ac*IDF, *enz*IDF, and *enz*SDF corresponded to strong C=O stretching vibration of hemicelluloses and lignin (Lin et al., 2019). Both these bands corroborate the higher degree of intermolecular hydrogen bonding and characteristic absorption of the benzene ring in lignin. C-H stretching band of hemicelluloses, cellulose, and asymmetric stretching vibration of methyl ester (pectin) at 1200-1400 cm^{-1} was observed in all the samples except *alk*SDF and *alk*IDF. A peak at 1009-1036 cm^{-1} was observed to be associated with pyranose, galactomannan, and pectins in all samples, except *enz*SDF, which had a peak at 1074 cm^{-1}, indicating stretching of C-O groups of carbohydrate (Cheng et al., 2017).

Further, X-ray diffraction determined the fractions' crystallinity index for in-depth characterization of the surface characteristics. The conclusions were drawn from the proven correlation between the peak intensity and crystallinity of the region, which subsequently represents higher tensile strength and hardness of the analyzed sample (Zheng et al., 2023). Fig. 1 illustrates the different 2θ values for each sample extracted through chemical-intensive approaches, which fall within the 17-45° range and confirm the presence of cellulose I crystal structure (Kaur et al., 2024). Conversely, *enz*SDF, *Uenz*SDF, and *enz*IDF had peaks at 2θ of 19.47, 20.09, and 23.47° (Fig. 1), representing the amorphous diffraction peaks of hemicelluloses and lignin (Zhang et al., 2023). The decrease in crystallinity by acid, enzyme, and ultrasonic treatment implies that some crystal regions were broken.

The thermal stabilities of all the fiber types were determined through differential scanning calorimetric (DSC) (Fig. 2). In the case of *ac*SDF and *ac*IDF, the peak temperature ranges from ~121 to 160 °C, primarily due to the evaporation of bound water (Menczel & Kohl, 2020). The second endothermic peak, ~250 °C in *ac*IDF, indicated the pyrolysis peak of pectin. The multi-stage thermal degradation values for *alk*SDF were 122.21 °C, 177.91 °C, and 139.56 °C for respective transition, onset, and end peak. However, similar values were significantly higher (>20 °C) for *alk*IDF, indicating the change in their pectin structure due

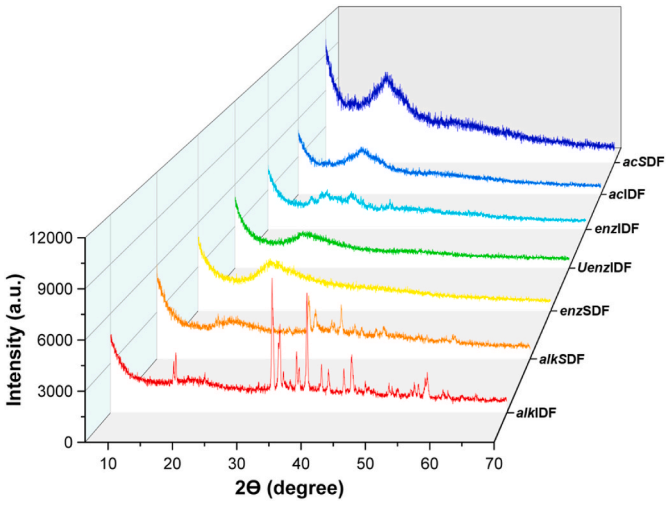

Fig. 1. X-Ray diffraction pattern of different fractions of dietary fibers extracted through various treatment methodologies.

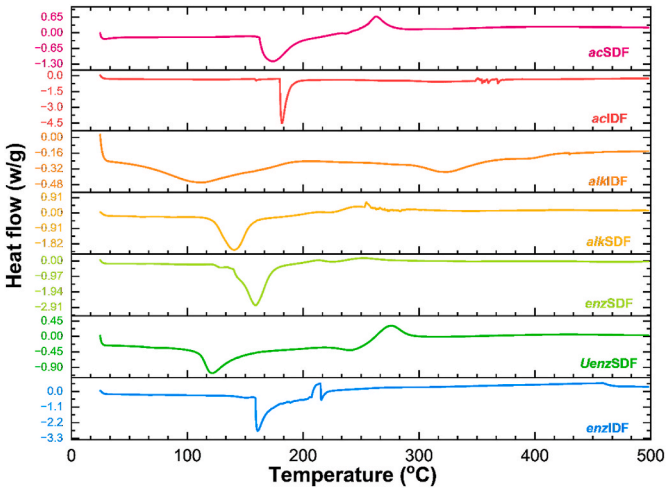

Fig. 2. Differential scanning calorimetry thermal pattern of dietary fibers extracted through different treatment methodologies.

to the relocation of bound water from the crystalline to an amorphous region (Ma et al., 2021). Similar conceptual details were corroborated by the calculated enthalpy (ΔH) values for *alk*SDF (265.70 J g^{-1}) and *alk*IDF (339.95 J g^{-1}). The higher enthalpy values can be attributed to the presence of a higher content of bound water.

The soluble (*enz*SDF) and insoluble (*enz*IDF) fractions of dietary fibers extracted through enzymatic methodologies exhibited peak temperature values of ~111.96 and 173.98 °C, respectively. These results (Fig. 2) indicated that the alkali and enzymatic treatment reduced the external and internal connection within the soluble dietary fibers. The exothermic peak above ~290 °C observed in the sample could be due to cellulose, hemicelluloses, and lignin pyrolysis. The peak temperature value for *Uenz*SDF (179.39 °C) is comparable to the peak temperature recorded (177.91 °C) for the *alk*SDF, indicating the similar thermal properties of the extracted fiber irrespective of the adopted methodology (Fig. 1). It is also an indicator of the efficiency of the enzyme combinations and ultrasonic pretreatment deployed for pearl millet preparation. However, the ΔH (159.56 J/g) for *Uenz*SDF is relatively low, indicating less severeness of the ultrasonic pretreatment than the chemical-intensive methodologies.

The SEM has revealed the topographical characteristics of all the extracted fibers. The dietary fibers obtained through the acid-intensive

approach resulted in smooth surface rheology (Fig. 3b) compared to the rough surface (Fig. 3c) of the soluble fraction extracted through the alkali-intensive approach. The observed surface smoothness after acid-driven methodology could be attributed to removing the lipids, crude proteins, and other components (Dong et al., 2020). In contrast, a significant loss of the polysaccharides due to the alkali-intensive method resulted in the observed surface roughness. Since both these methodologies resulted in irregular massive surfaces, indicating more hydrophilic and lipophilic groups exposed to the surface. A compact thread-like surface with large pores (Fig. 3a–d) in the *alk*SDF and *ac*SDF case indicates that starch and protein were removed completely (Fig. 3). Additionally, these cavities provide a larger surface within the internal areas of soluble dietary fiber. Contrarily to soluble fiber characteristics, both acid and alkali-intensive methodologies significantly impacted the insoluble fractions, resulting in the fragmented thread-like structure with irregular topology. This could be attributed to the loosening of the tightly packed structure of insoluble fractions due to the detrimental impacts of the chemical-intensive methodologies. The impacts of the enzymatic methodologies are relatively mild over the topological characteristics of both the soluble and insoluble fractions of the dietary fibers.

3.3. Characterization of functional properties

A myriad of analytical and biochemical tests were carried out to investigate the functional characteristics of the extracted dietary fibers. The initial characterization includes the determination of the water-holding (WHC) and oil-holding (OLC) capacities—an indicator of nutrients released and the life of the fiber. In the present case, the WHC of the dietary fibers ranges from 1.01 to 9.22 g/g (Fig. S3). The fiber extracted as *alk*SDF exhibited the highest WHC (9.22 g/g) compared to the lowest values (1.01 g/g) observed for the *enz*SDF. The soluble fractions of the dietary fibers exhibited higher WHC values over their insoluble counterparts due to the structural compactness of the later fiber types (Lin et al., 2019). However, the dietary fibers extracted through the enzymatic methodologies are an exception to this observation. The lower WHC values for the enzymatically extracted fibers compared to the other methods could be attributed to the starch loss catalyzed by the α-amylase treatment (Skowron et al., 2020).

The OHC represents the fiber's ability to absorb fat and prevent its loss during processing. Therefore, an inverse OHC data pattern was recorded and compared to WHC for *alk*SDF and *enz*SDF. The lowest value observed for the *alk*SDF (Fig. S3), could be attributed to the presence of lignin and other hydrophobic components of fibers (Gómez-Ordóñez et al., 2010). A similar trend was observed for the swelling capacity (SC), which represents the ratio of fiber's volume to weight after being immersed in water. Higher SC values are desirable as they are an important indicator of food functionality and can help prevent food from shrinking, thus making them highly desirable for the food processing industry. The highest SC value of the *alk*SDF could be attributed to the deeper penetration into the fiber, which exposed many water absorption sites (Fig. S2) (Ma et al., 2021).

CAC, specifically for the soluble dietary fiber fractions, holds enormous biomedical potential as it can reduce the cholesterol amount absorbed into the bloodstream by binding to it in the intestines, thus preventing cholesterol accumulation in arteries. Therefore, high CAC values for the extracted dietary fiber soluble fractions are desirable. Notably higher CAC values were observed for *ac*SDF and *alk*SDF over their insoluble counterparts, confirming the biomedical potential of the extracted dietary fibers (Fig. 4). The SEM images (Fig. 3) further corroborated the observed CAC values, confirming the soluble fractions' loosened structure and larger surface area. In the case of enzymatic approach, the CAC values were comparable for both soluble and insoluble fractions of the dietary fibers (Fig. 4). However, for the *Uenz*SDF, a significant reduction in the CAC value was observed. It might be due to the damaged functional groups interacting with the cholesterol molecule for its absorption resulting from the ultrasonication.

The soluble fractions are also reported to regulate postprandial serum glucose through binding with the released sugars from carbohydrate-rich diets. Dietary fibers can bind glucose within intestinal juice and may lower the postprandial serum glucose. Unlike CAC, the highest value for the GAC was observed for the *enz*SDF fraction (Fig. 4).

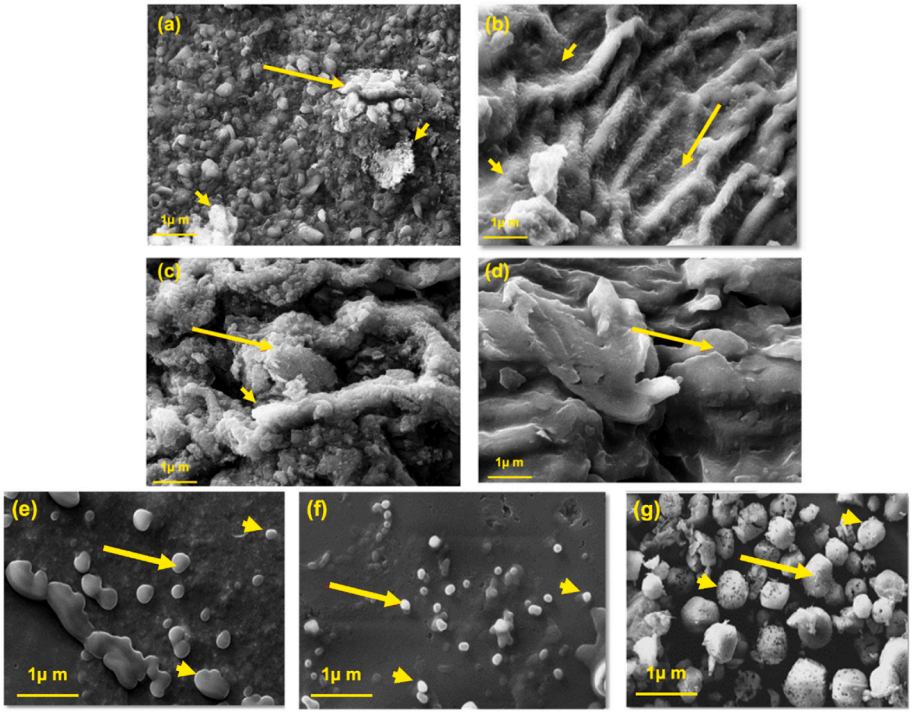

Fig. 3. Scanning electron micrographs exhibit surface roughness, cavities present, and granular materials, enhancing the strength properties of dietary fibers extracted from the pearl millet.

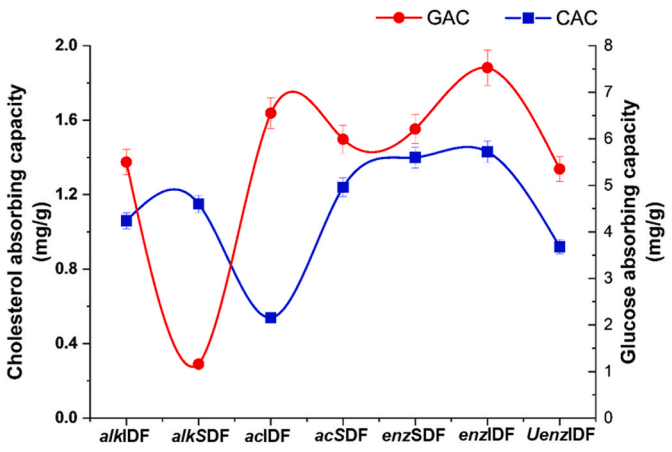

Fig. 4. Determination of biomedical characteristics of the dietary fiber extracted through various chemical-intensive and enzymatic approaches from pearl millet.

The extreme variations in the enzSDF characteristics towards CAC and GAC could be attributed to the preference of the polar/non-polar groups of the cholesterol and hydrophilic characteristics of the glucose towards the swollen surface of the enzSDF. Similar mechanisms have been reported for the GAC properties exhibited by the kiwifruit-derived dietary fiber (Wang et al., 2021).

The HPLC-based identification protocols were followed for qualitative analysis of various phenolic compounds present in the soluble fractions of the dietary fiber. Based on the reported details (Ogunsina, 2020), the key phenolic compounds identified in the enzymatically treated sample is given in Fig. 5. The remarkable presence of vanillic acid (RT 11.598) and *p*-hydroxybenzoic acid (RT 12.489) also corroborated our hypothesis on the anti-inflammatory characteristics of the fiber extracted from the pearl millet and made it one of the suitable candidates for biomedical applications. The presence of cinnamic acid (RT 9.253) can be attributed to the aroma of the dietary fiber and is also reported for the diabetes treatments (Ruwizhi & Aderibigbe, 2020). Likewise, the presence of gentinsic acid (RT 10.085) confirmed the anti-inflammatory, antirheumatic, and anti-arthritic characteristics of the enzymatically extracted fiber (Mardani-Ghahfarokhi & Farhoosh, 2020). It is also reported to inhibit LDL oxidation and lipid hydroperoxide formation in human plasma. However, a few minor peaks remain unidentified due to low threshold concentrations for their extraction for subsequent validation.

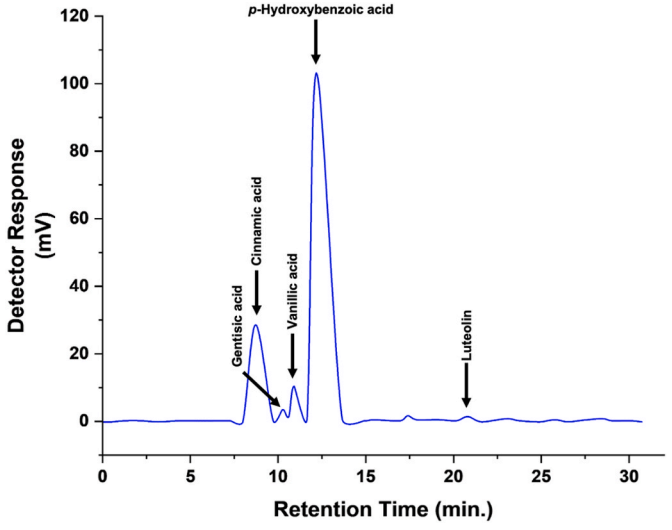

Fig. 5. Chromatogram validating the phenolic compounds of fiber. The retention time of the compounds is similar to the extracted phenolics reported for the pearl millet.

The antioxidant activities of extracted fractions were determined through free radical scavenging activities using standard ABTS and FRAP assays (Fig. 6). The higher percentage of inhibition indicated an increased ability to donate hydrogen governing antioxidant activity. The highest ABTS free radical scavenging activity (92%) was observed for *alk*SDF in contrast to *enz*IDF, which exhibited the least antioxidant characteristics (11%). In the case of the FRAP assay, *Uenz*SDF exhibited the highest activity (87%), and the least was observed with the *enz*IDF (29%). The antioxidant activity of soluble fractions was higher than their insoluble counterparts. This could be attributed to bound phenolic compounds with other structural constituents, e.g., hemicelluloses. A similar observation was reported that the antioxidant activity of foxtail millet bran SDF was higher than that of IDF (Dong et al., 2008). The improved antioxidant characteristics of the *Uenz*SDF fraction could be hypothesized by enhanced release of phenolic compounds governing free radical scavenging activities.

The ability of the extracted fraction to enhance the growth of probiotic culture was determined in terms of the prebiotic index, which is the ratio of the growth of probiotics in the tested dietary fiber fraction to the growth of probiotics in a controlled carbohydrate (inulin). A value of PI > 1.0 indicates the substrate's positive effect on probiotics' growth. In contrast, PI < 1.0 indicated low effectiveness of the tested fiber (Fidriyanto et al., 2023). The prebiotic assessments of extracted fractions on the growth of the probiotic strain of *L. rhamnosus* GG in MRS broth were lowest for *ac*SDF and highest for *alk*SDF. These results indicated a significantly higher PI value for dietary fibers extracted through alkaline and enzymatic methodologies. Contrarily, the acid treatment could might have damaged the structure of fibers serving as prebiotic components (e.g., oligosaccharides), resulting in lower PI values. The difference among these extracted fractions could be attributed to the presence of specific metabolic enzymes and transport systems within the bacterial cultures. Moreover, the acid treatment might have induced degradation of potential other prebiotic components during processing of the fiber fraction.

3.4. In-silico analysis

The 3D structure of α-amylglucosidase was modeled using homology-based techniques (Basotraet al., 2019). Position-Specific Iterative Basic Local Alignment Search Tool (PSI-BLAST) was employed to identify homologous protein structures, and the top five matches, with PDB IDs: 6FRV, 1GAI, 6FHV, 2VN4, and 6FHW, were selected as templates. The sequence identity and similarity with these

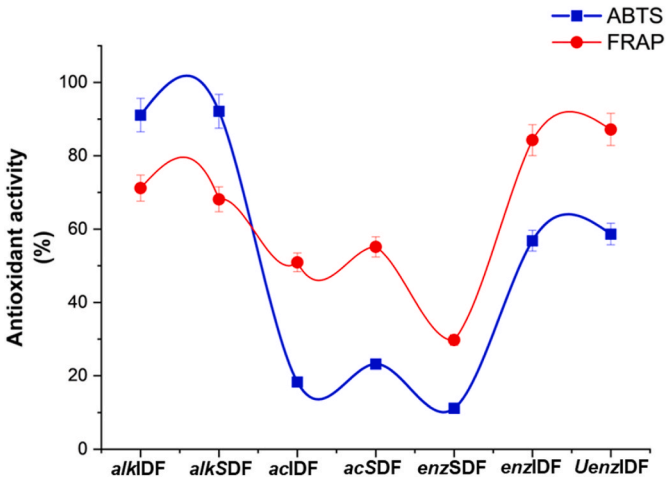

Fig. 6. Quantitative representation of the antioxidant activities observed for the extracted dietary fiber as measured using ABTS and FRAP assay.

templates were 31.3% and 20.1%, respectively. Based on these templates, five homology models were generated, and the model with the lowest DOPE score (−70166.164) and the most favorable PDF energy (−13720.17) was selected for further analysis. Structural alignment of the selected model with the 6FRV template was performed, and root mean square deviation (RMSD) analysis was carried out using C-alpha atoms. This analysis yielded an RMSD of 1.26 Å, indicating a high degree of structural conservation between the model and the template and supporting the reliability of the homology model (Fig. S4a). A Ramachandran plot was generated (Fig. S4b) to assess the stereochemical quality of the model. More than 95% of residues were found to be in the acceptable regions, which signifies the appropriateness of the modeled structure and is consistent with a well-folded protein structure. The Profile-3D score for the amylglucosidase model was 238.86, out of a maximum expected score of 281.96. This score is notably higher than the 190.64 observed for the 2CDU template, further confirming the high quality and structural reliability of the derived amylglucosidase model. Finally, structural validation using the PROCHECK program confirmed that the overall protein fold met the expected quality standards.

The docking process yielded a CDOCKER energy of −40.505 kcal/mol. The lowest energy docking position was selected for further analysis. The binding energy of the ligand-receptor complex was determined to be −101.8434 kcal/mol, with a total complex energy of 17065.51 kcal/mol. The catalytic center of glucoamylase, shown in this structure, provides insight into the detailed interactions between the enzyme and its amylase substrate (Fig. S4c). Key residues like Asp136 (D136), Thr638 (T638), Asp584 (D584), and Asp637 (D637) are strategically positioned to interact with the substrate through a series of hydrogen bonds, which stabilize the substrate within the binding pocket and align it for catalytic hydrolysis (Fig. S4d). The amylase substrate forms direct hydrogen bonds with Asp584, Thr638, and Asp637, suggesting that these residues play an essential role in anchoring the substrate. In particular, Asp637 appears to be in close proximity to the substrate's glycosidic bonds. Additional stabilization is provided by residues such as Trp587 (W587) and Tyr588 (Y588), which are involved in van der Waals interactions that further anchor the substrate. Val589 (V589) and Thr634 (T634) also contribute through non-covalent interactions, maintaining the structural integrity of the enzyme-substrate complex. The secondary structure elements surrounding the active site, such as α-helices (red) and β-sheets (cyan), create a confined environment that limits substrate movement, directing it toward catalytically active residues. This structural arrangement ensures that the substrate is correctly oriented, maximizing the efficiency of the hydrolysis reaction.

4. Conclusions

Despite the immense potential of bioactive components in millet, further exploration is needed for it to be utilized as a major food grain in society. Due to the nutraceutical potential of the fibers and their economic implications, the impact of various extraction methods on the yield and activity of dietary fibers from pearl millet flour has been reported. The extraction method significantly influences the yield and physicochemical characteristics of the fiber components. Alkali treatment led to higher yields and enhanced functional activities, such as increased prebiotic activities. The green route using ultrasonication followed by enzymatic-assisted extraction did not improve yield, rheological characteristics, or other functional activities, except for enhanced glucose absorption capacity and cholesterol-lowering properties. Based on the physicochemical and functional characteristics of fibers from pearl millet, it can be concluded that these fibers can be incorporated into different food matrices to enhance texture and rheological qualities. These findings support the potential of pearl millet fiber as a functional ingredient, however futher beneficial effects on structural and functional diversity of gut microbiota can be tested using in vivo models.

CRediT authorship contribution statement

K.M. Manju: Writing – original draft, Investigation, Data curation. **Swati Srivastava:** Data curation. **Brij Pal Singh:** Writing – original draft, Investigation, Formal analysis, Data curation. **Dheeraj Raya:** Formal analysis, Data curation. **Rohit:** Investigation. **Rusli Fridyanto:** Writing – review & editing, Writing – original draft, Formal analysis. **Roni Ridwan:** Writing – review & editing, Writing – original draft, Formal analysis. **Yantyati Widyastuti:** Writing – original draft, Formal analysis. **Teck Chwen Loh:** Writing – original draft, Formal analysis. **Hooi Ling Foo:** Writing – review & editing, Writing – original draft, Formal analysis. **Saurabh Sudha Dhiman:** Writing – review & editing, Supervision, Investigation, Funding acquisition. **Gunjan Goel:** Writing – review & editing, Writing – original draft, Supervision, Investigation, Funding acquisition, Conceptualization.

Declaration of competing interest

The authors declare that they have no conflict of interest.

Acknowledgments

The authors acknowledge Science and Engineering Research Board (File No. IMRC/AISTDF/CRD/2019/000181) for funding the research. SSD acknowledges financial support provided by the NSF award # 1849206.

Appendix A. Supplementary data

Supplementary data to this article can be found online at https://doi.org/10.1016/j.fbio.2025.106318.

Data availability

Data will be made available on request.

References

Agrawal, H., Joshi, R., & Gupta, M. (2016). Isolation, purification and characterization of antioxidative peptide of pearl millet (Pennisetum glaucum) protein hydrolysate. *Food Chemistry, 204*, 365–372. https://doi.org/10.1016/j.foodchem.2016.02.127

Agrawal, P., Singh, B. R., Gajbe, U., Kalambe, M. A., & Bankar, M. (2023). Managing diabetes mellitus with millets: A new solution. *Cureus, 15*(9), Article e44908. https://doi.org/10.7759/cureus.44908

Asp, N. G. (1987). Dietary fibre-definition, chemistry and analytical determination. *Molecular Aspects of Medicine, 9*(1), 17–29. https://doi.org/10.1016/0098-2997(87)90014-8

Bader Ul Ain, H., Saeed, F., Khan, M. A., Niaz, B., Khan, S. G., Anjum, F. M., Tufail, T., & Hussain, S. (2019). Comparative study of chemical treatments in combination with extrusion for the partial conversion of wheat and sorghum insoluble fiber into soluble. *Food Science and Nutrition, 7*(6), 2059–2067. https://doi.org/10.1002/fsn3.1041

Bala Durairajan, M., Velavan Sundararajan, V., Kannan, G., Mathews Paul, B., Muniyandi, K., & Thangaraj, P. (2024). Elicitation of nutritional, antioxidant, and antidiabetic potential of barnyard millet (Echinochloa esculenta (A. Braun) H. Scholz) sprouts and microgreens through in vitro bio-accessibility assessment. *Food Chemistry, 441*, Article 138282. https://doi.org/10.1016/j.foodchem.2023.138282

Basotra, N., Dhiman, S. S., Agrawal, D., Sani, R. K., Tsang, A., & Chadha, B. S. (2019). Characterization of a novel Lytic Polysaccharide Monooxygenase from Malbranchea cinnamomea exhibiting dual catalytic behavior. *Carbohydrate Research, 478*, 46–53. https://doi.org/10.1016/j.carres.2019.04.006

Benzie, I. F. F., & Strain, J. J. (1996). The ferric reducing ability of plasma (FRAP) as a measure of "antioxidant power": The FRAP assay. *Analytical Biochemistry, 239*, 70–76. https://doi.org/10.1006/abio.1996.0292

Buljeta, I., Šubarić, D., Babić, J., Pichler, A., Šimunović, J., & Kopjar, M. (2023). Extraction of dietary fibers from plant-based industry waste: A comprehensive review. *Applied Sciences, 13*(16), 9309. https://doi.org/10.3390/app13169309

Calcio Gaudino, E., Grillo, G., Tabasso, S., Stevanato, L., Cravotto, G., Marjamaa, K., Pihlajaniemi, V., Koivula, A., Aro, N., & Uusitalo, J. (2022). Optimization of ultrasound pretreatment and enzymatic hydrolysis of wheat straw: From lab to semi-industrial scale. *Journal of Cleaner Production, 380*, Article 134897. https://doi.org/10.1016/j.jclepro.2022.134897

Chandrasekara, A., & Shahidi, F. (2011). Determination of antioxidant activity in free and hydrolyzed fractions of millet grains and characterization of their phenolic

profiles by HPLC-DAD-ESI-MSn. *Journal of Functional Foods, 3*(3), 144–158. https://doi.org/10.1016/j.jff.2011.03.007
Cheng, L., Zhang, X., Hong, Y., Li, Z., Li, C., & Gu, Z. (2017). Characterisation of physicochemical and functional properties of soluble dietary fibre from potato pulp obtained by enzyme-assisted extraction. *International Journal of Biological Macromolecules, 101*, 1004–1011. https://doi.org/10.1016/j.ijbiomac.2017.03.156
Chylińska, M., Szymańska-Chargot, M., Kruk, B., & Zdunek, A. (2016). Study on dietary fibre by Fourier transform-infrared spectroscopy and chemometric methods. *Food Chemistry, 196*, 114–122. https://doi.org/10.1016/j.foodchem.2015.09.029
Coppin, J. P., Xu, Y., Chen, H., Pan, M.-H., Ho, C.-T., Juliani, R., Simon, J. E., & Wu, Q. (2013). Determination of flavonoids by LC/MS and anti-inflammatory activity in Moringa oleifera. *Journal of Functional Foods, 5*(4), 1892–1899. https://doi.org/10.1016/j.jff.2013.09.010
de Simas, K. N., Vieira, L.d. N., Podestá, R., Vieira, M. A., Rockenbach, I. I., Petkowicz, C. L. O., de Deus Medeiros, J., de Francisco, A., Amante, E. R., & Amboni, R. D. M. C. (2010). Microstructure, nutrient composition and antioxidant capacity of king palm flour: A new potential source of dietary fibre. *Bioresource Technology, 101*(14), 5701–5707. https://doi.org/10.1016/j.biortech.2010.02.053
Devi, P. B., Vijayabharathi, R., Sathyabama, S., Malleshi, N. G., & Priyadarisini, V. B. (2014). Health benefits of finger millet (eleusine coracana L.) polyphenols and dietary fiber: A review. *Journal of Food Science and Technology, 51*(6), 1021–1040. https://doi.org/10.1007/s13197-011-0584-9
Dhiman, S. S., Selvaraj, C., Li, J., Singh, R., Zhao, X., Kim, D., Kim, J. Y., Kang, Y. C., & Lee, J. K. (2016). Phytoremediation of metal-contaminated soils by the hyperaccumulator canola (Brassica napus L.) and the use of its biomass for ethanol production. *Fuel, 183*, 107–114. https://doi.org/10.1016/j.fuel.2016.06.025
Dhiman, S. S., Zhao, X., Li, J., Kim, D., Kalia, V. C., Kim, I.-W., Kim, J. Y., & Lee, J. K. (2017). Metal accumulation by sunflower (Helianthus annuus L.) and the efficacy of its biomass in enzymatic saccharification. *PLoS One, 12*(4), Article e0175845. https://doi.org/10.1371/journal.pone.0175845
Dhingra, D., Michael, M., Rajput, H., & Patil, R. T. (2012). Dietary fibre in foods: A review. *Journal of Food Science and Technology, 49*(3), 255–266. https://doi.org/10.1007/s13197-011-0365-5
Ding, Q., Li, Z., Wu, W., Su, Y., Sun, N., Luo, L., Ma, H., & He, R. (2020). Physicochemical and functional properties of dietary fiber from nannochloropsis oceanica: A comparison of alkaline and ultrasonic-assisted alkaline extractions. *Lebensmittel-Wissenschaft & Technologie, 133*, Article 110080. https://doi.org/10.1016/j.lwt.2020.110080
Dong, W., Wang, D., Hu, R., Long, Y., & Lv, L. (2020). Chemical composition, structural and functional properties of soluble dietary fiber obtained from coffee peel using different extraction methods. *Food Research International, 136*, Article 109497. https://doi.org/10.1016/j.foodres.2020.109497
Dong, T., Xia, R., Wang, M., Xiao, Z., & Liu, P. (2008). Changes in dietary fibre, polygalacturonase, cellulase of navel orange (Citrus sinensis (L.) Osbeck 'Cara Cara') fruits under different storage conditions. *Scientia Horticulturae, 116*(4), 414–420. https://doi.org/10.1016/j.scienta.2008.03.006
Elsafy, M., Othman, M. H., Hassan, A. B., Elkhatim, K. A. S., Hamid, M. G., Rahmatov, M., & Abdelhalim, T. S. (2024). Phytochemical components and antioxidant properties of traditional Sudanese pearl millet non-alcoholic drink. *Food Chemistry Advances, 5*, Article 100739. https://doi.org/10.1016/j.focha.2024.100739
Feng, X., Ameer, K., Jiang, G., & Ramachandraiah, K. (2024). Effects of extraction methods on the structural characteristics and functional properties of dietary fiber extracted from papaya peel and seed. *Frontiers in Sustainable Food Systems, 8*, Article 1340961. https://doi.org/10.3389/fsufs.2024.1340961
Fidriyanto, R., Juanssilfero, A. B., Sarwono, K. A., Ridwan, R., Nahrowi, N., & Jayanegara, A. (2024). Enhancing physicochemical, rheological properties, and in vitro rumen fermentation of starch with D. Don fruit extract. *Animal Science Journal, 95*(1), Article e13950. https://doi.org/10.1111/asj.13950
Fidriyanto, R., Singh, B. P., Manju, K. M., Widyastuti, Y., & Goel, G. (2023). Multivariate analysis of structural and functional properties of fibres from apple pomace using different extraction methods. *Food Production, Processing and Nutrition, 5*(1), 6. https://doi.org/10.1186/s43014-022-00119-8
Gómez-Ordóñez, E., Jiménez-Escrig, A., & Rupérez, P. (2010). Dietary fibre and physicochemical properties of several edible seaweeds from the northwestern Spanish coast. *Food Research International, 43*(9), 2289–2294. https://doi.org/10.1016/j.foodres.2010.08.005
Happi Emaga, T., Robert, C., Ronkart, S. N., Wathelet, B., & Paquot, M. (2008). Dietary fibre components and pectin chemical features of peels during ripening in banana and plantain varieties. *Bioresource Technology, 99*(10), 4346–4354. https://doi.org/10.1016/j.biortech.2007.08.030
Hilu, K. W., De Wet, J. M. J., & Seigler, D. (1978). Flavonoid patterns and systematics in Eleusine. *Biochemical Systematics and Ecology, 6*(3), 247–249. https://doi.org/10.1016/0305-1978(78)90013-3
Jagtap, S. S., Dhiman, S. S., Kim, T. S., Kim, I. W., & Lee, J. K. (2014). Characterization of a novel endo-β-1,4-glucanase from Armillaria gemina and its application in biomass hydrolysis. *Applied Microbiology and Biotechnology, 98*(2), 661–669. https://doi.org/10.1007/s00253-013-4894-x
Jagtap, S. S., Dhiman, S. S., Kim, T.-S., Li, J., Chan Kang, Y., & Lee, J. K. (2013). Characterization of a β-1,4-glucosidase from a newly isolated strain of Pholiota adiposa and its application to the hydrolysis of biomass. *Biomass and Bioenergy, 54*, 181–190. https://doi.org/10.1016/j.biombioe.2013.03.032
Jia, F., Liu, X., Gong, Z., Cui, W., Wang, Y., & Wang, W. (2020). Extraction, modification, and property characterization of dietary fiber from Agrocybe cylindracea. *Food Science and Nutrition, 8*(11), 6131–6143. https://doi.org/10.1002/fsn3.1905
Kalyani, D., Dhiman, S. S., Kim, H., Jeya, M., Kim, I. W., & Lee, J. K. (2012). Characterization of a novel laccase from the isolated Coltricia perennis and its application to detoxification of biomass. *Process Biochemistry, 47*(4), 671–678. https://doi.org/10.1016/j.procbio.2012.01.013
Karimi, R., Azizi, M. H., Xu, Q., Sahari, M. A., & Hamidi, Z. (2018). Enzymatic removal of starch and protein during the extraction of dietary fiber from barley bran. *Journal of Cereal Science, 83*, 259–265. https://doi.org/10.1016/j.jcs.2018.07.012
Kaur, R., Panesar, P. S., Kaur, B., & Riar, C. S. (2024). Hydrothermal extraction of dietary fiber from pearl millet bran: Optimization, physico-chemical, structural and functional characterization. *Journal of Food Science and Technology, 61*(8), 1536–1546. https://doi.org/10.1007/s13197-023-05921-x
Lin, Y., Chen, K., Tu, D., Yu, X., Dai, Z., & Shen, Q. (2019). Characterization of dietary fiber from wheat bran (Triticum aestivum L.) and its effect on the digestion of surimi protein. *Lebensmittel-Wissenschaft & Technologie, 102*, 106–112. https://doi.org/10.1016/j.lwt.2018.12.024
Lin, H. H., Lin, K. H., Yang, M. J., Nguyen, H. C., Wang, H. J., Huang, H. X., & Huang, M. Y. (2022). Physiological responses and antioxidant properties of coriander plants (Coriandrum sativum L.) under different light intensities of red and blue lights. *Scientific Reports, 12*(1), Article 21139. https://doi.org/10.1038/s41598-022-25749-3
Liu, X., Liu, S., Xi, H., Xu, J., Deng, D., & Huang, G. (2019). Effects of soluble dietary fiber on the crystallinity, pasting, rheological, and morphological properties of corn resistant starch. *Lebensmittel-Wissenschaft & Technologie, 111*, 632–639. https://doi.org/10.1016/j.lwt.2019.01.059
Lovegrove, A., Edwards, C. H., De Noni, I., Patel, H., El, S. N., Grassby, T., Zielke, C., Ulmius, M., Nilsson, L., & Butterworth, P. J. (2017). Role of polysaccharides in food, digestion, and health. *Critical Reviews in Food Science and Nutrition, 57*(2), 237–253. https://doi.org/10.1080/10408398.2014.939263
Ma, R., Chen, J.-N., Zhou, X.-j., Lin, H., Gao, Q., Peng, X., Tanokura, M., & Xue, Y. (2021). Effect of chemical and enzymatic modifications on the structural and physicochemical properties of dietary fiber from purple turnip (Brassica rapa L.). *Lebensmittel-Wissenschaft & Technologie, 145*, Article 111313. https://doi.org/10.1016/j.lwt.2021.111313
Mardani-Ghahfarokhi, A., & Farhoosh, R. (2020). Antioxidant activity and mechanism of inhibitory action of gentisic and α-resorcylic acids. *Scientific Reports, 10*(1), Article 19487. https://doi.org/10.1038/s41598-020-76620-2
Menczel, J. D., & Kohl, W. S. (2020). Differential scanning calorimetry (DSC) in fiber research. In M. Jaffe, & J. D. Menczel (Eds.), *Thermal analysis of textiles and fibers* (pp. 17–69). Woodhead Publishing.
Ogunsina, O. (2020). The synergistic interaction of phenolic compounds in pearl millets with respect to antioxidant and antimicrobial properties. *American Journal of Food Science and Health, 6*(3), 80–88.
Okrathok, S., Thumanu, K., Pukkung, C., Molee, W., & Khempaka, S. (2022). Extraction of dietary fibers from cassava pulp and cassava distiller's dried grains and assessment of their components using Fourier transform infrared spectroscopy to determine their further use as a functional feed in animal diets. *Animal Bioscience, 35*(7), 1048–1058. https://doi.org/10.5713/ab.21.0430
Palafox-Carlos, H., Ayala-Zavala, J. F., & González-Aguilar, G. A. (2011). The role of dietary fiber in the bioaccessibility and bioavailability of fruit and vegetable antioxidants. *Journal of Food Science, 76*(1), R6–r15. https://doi.org/10.1111/j.1750-3841.2010.01957.x
Pattanashetti, S. K., Upadhyaya, H. D., Dwivedi, S. L., Vetriventhan, M., & Reddy, K. N. (2016). Pearl millet. In M. Singh, & H. D. Upadhyaya (Eds.), *Genetic and genomic resources for grain cereals improvement* (pp. 253–289). Academic Press.
Pei, J., Umapathy, V. R., Vengadassalapathy, S., Hussain, S. F. J., Rajagopal, P., Jayaraman, S., Veeraraghavan, V. P., Palanisamy, C. P., & Gopinath, K. (2022). A review of the potential consequences of pearl millet (Pennisetum glaucum) for diabetes mellitus and other biomedical applications. *Nutrients, 14*(14), 2932. https://doi.org/10.3390/nu14142932
Raya, D., Militello, K., Gadhamshetty, V., & Dhiman, S. (2023). Nanowire Formation in sulfate-reducing bacteria under stress conditions. In , *Vol. 1434. Microbial stress response: Mechanisms and data science, ACS symposium series* (pp. 59–73). American Chemical Society.
Raya, D., Shreya, A., Kumar, A., Giri, S. K., Salem, D. R., Gnimpieba, E. Z., Gadhamshetty, V., & Dhiman, S. S. (2022). Molecular regulation of conditioning film formation and quorum quenching in sulfate reducing bacteria. *Frontiers in Microbiology, 13*, Article 1008536. https://doi.org/10.3389/fmicb.2022.1008536
Research, P. (2024). Dietary fibers market size, share, and trends 2024 to 2034. https://www.precedenceresearch.com/dietary-fibers-market.
Robertson, J. A., de Monredon, F. D., Dysseler, P., Guillon, F., Amado, R., & Thibault, J. F. (2000). Hydration properties of dietary fibre and resistant starch: A European collaborative study. *Lebensmittel-Wissenschaft & Technologie, 33*(2), 72–79. https://doi.org/10.1006/fstl.1999.0595
Ruwizhi, N., & Aderibigbe, B. A. (2020). Cinnamic acid derivatives and their biological efficacy. *International Journal of Molecular Sciences, 21*(16), 5712. https://doi.org/10.3390/ijms21165712
Selvaraj, C., Krishnasamy, G., Jagtap, S. S., Patel, S. K. S., Dhiman, S. S., Kim, T. S., Singh, S. K., & Lee, J. K. (2016). Structural insights into the binding mode of d-sorbitol with sorbitol dehydrogenase using QM-polarized ligand docking and molecular dynamics simulations. *Biochemical Engineering Journal, 114*, 244–256. https://doi.org/10.1016/j.bej.2016.07.008
Skowron, P. M., Krawczun, N., Żebrowska, J., Krefft, D., Żołnierkiewicz, O., Bielawa, M., Jeżewska-Frąckowiak, J., Janus, Ł., Witkowska, M., & Palczewska, M. (2020). An efficient method for the construction of artificial, concatemeric DNA, RNA and proteins with genetically programmed functions, using a novel, vector-enzymatic DNA fragment amplification-expression technology. *MethodsX, 7*, Article 101070. https://doi.org/10.1016/j.mex.2020.101070

Sofi, S. A., Ahmed, N., Farooq, A., Rafiq, S., Zargar, S. M., Kamran, F., Dar, T. A., Mir, S. A., Dar, B. N., & Mousavi Khaneghah, A. (2023). Nutritional and bioactive characteristics of buckwheat, and its potential for developing gluten-free products: An updated overview. *Food Science and Nutrition, 11*(5), 2256–2276. https://doi.org/10.1002/fsn3.3166

Subba Rao, M. V., & Muralikrishna, G. (2002). Evaluation of the antioxidant properties of free and bound phenolic acids from native and malted finger millet (ragi, Eleusine coracana Indaf-15). *Journal of Agricultural and Food Chemistry, 50*(4), 889–892. https://doi.org/10.1021/jf011210d

Tejada-Ortigoza, V., Garcia-Amezquita, L. E., Torres, J. A., & Welti-Chanes, J. (2020). Chemical processes for the extraction and modification of dietary fiber. In J. Welti-Chanes, S. O. Serna-Saldívar, O. Campanella, & V. Tejada-Ortigoza (Eds.), *Science and technology of fibers in food systems* (pp. 343–361). Springer International Publishing.

Tolve, R., Zanoni, M., Ferrentino, G., Gonzalez-Ortega, R., Sportiello, L., Scampicchio, M., & Favati, F. (2024). Dietary fibers effects on physical, thermal, and sensory properties of low-fat ice cream. *Lebensmittel-Wissenschaft & Technologie, 199*, Article 116094. https://doi.org/10.1016/j.lwt.2024.116094

Vijayakumar, B. G., Ramesh, D., Joji, A., Jayachandra Prakasan, J., & Kannan, T. (2020). In silico pharmacokinetic and molecular docking studies of natural flavonoids and synthetic indole chalcones against essential proteins of SARS-CoV-2. *European Journal of Pharmacology, 886*, Article 173448. https://doi.org/10.1016/j.ejphar.2020.173448

Wang, S., Fang, Y., Xu, Y., Zhu, B., Piao, J., Zhu, L., Yao, L., Liu, K., Wang, S., & Zhang, Q. (2022). The effects of different extraction methods on physicochemical, functional and physiological properties of soluble and insoluble dietary fiber from Rubus chingiiHu. fruits. *Journal of Functional Foods, 93*, Article 105081. https://doi.org/10.1016/j.jff.2022.105081

Wang, K., Guo, J., Cheng, J., Zhao, X., Ma, B., Yang, X., & Shao, H. (2021). Ultrasound-assisted extraction of polysaccharide from spent Lentinus edodes substrate: Process optimization, precipitation, structural characterization and antioxidant activity. *International Journal of Biological Macromolecules, 191*, 1038–1045. https://doi.org/10.1016/j.ijbiomac.2021.09.174

Wang, C., Song, R., Wei, S., Wang, W., Li, F., Tang, X., & Li, N. (2020). Modification of insoluble dietary fiber from ginger residue through enzymatic treatments to improve its bioactive properties. *Lebensmittel-Wissenschaft & Technologie, 125*, Article 109220. https://doi.org/10.1016/j.lwt.2020.109220

Yang, Y.-y., Ma, S., Wang, X.-x., & Zheng, X.-l. (2017). Modification and application of dietary fiber in foods. *Journal of Chemistry, 1*, Article 9340427. https://doi.org/10.1155/2017/9340427

Zhang, S., Xu, X., Cao, X., & Liu, T. (2023). The structural characteristics of dietary fibers from Tremella fuciformis and their hypolipidemic effects in mice. *Food Science and Human Wellness, 12*(2), 503–511. https://doi.org/10.1016/j.fshw.2022.07.052

Zheng, Y., Li, J., Wang, X., Guo, M., Cheng, C., & Zhang, Y. (2023). Effects of three biological combined with chemical methods on the microstructure, physicochemical properties and antioxidant activity of millet bran dietary fibre. *Food Chemistry, 411*, Article 135503. https://doi.org/10.1016/j.foodchem.2023.135503